Synthesis, structures and catalytic activity of 1,3-bis(aryl)triazenide(*p*-cymene)ruthenium(II) complexes

Erick Correa-Ayala, Aida Valle-Delgado, Gustavo Ríos-Moreno, Daniel Chávez, David Morales-Morales, Simón Hernández-Ortega, Juventino García, Marco Flores-Álamo, Valentín Miranda-Soto, Miguel Parra-Hake

PII: S0020-1693(16)30096-2
DOI: http://dx.doi.org/10.1016/j.ica.2016.03.004
Reference: ICA 16939

To appear in: *Inorganica Chimica Acta*

Received Date: 13 January 2016
Revised Date: 1 March 2016
Accepted Date: 3 March 2016

Please cite this article as: E. Correa-Ayala, A. Valle-Delgado, G. Ríos-Moreno, D. Chávez, D. Morales-Morales, S. Hernández-Ortega, J. García, M. Flores-Álamo, V. Miranda-Soto, M. Parra-Hake, Synthesis, structures and catalytic activity of 1,3-bis(aryl)triazenide(*p*-cymene)ruthenium(II) complexes, *Inorganica Chimica Acta* (2016), doi: http://dx.doi.org/10.1016/j.ica.2016.03.004

Synthesis, structures and catalytic activity of 1,3-bis(aryl)triazenide(*p*-cymene)ruthenium(II) complexes

Erick Correa-Ayala[a], Aida Valle-Delgado[a], Gustavo Ríos-Moreno[b], Daniel Chávez[a], David Morales-Morales[c], Simón Hernández-Ortega[c], Juventino García[d], Marco Flores-Álamo[d], Valentín Miranda-Soto[a,*], Miguel Parra-Hake[a,*]

[a] *Centro de Graduados e Investigación, Instituto Tecnológico de Tijuana, Apartado Postal 1166, Tijuana, B.C. 22000, México*
[b] *Unidad Académica de Ciencias Químicas, Universidad Autónoma de Zacatecas, Campus Siglo XXI. Carretera a Guadalajara Km. 6, Ejido La Escondida, Zacatecas 98160, México*
[c] *Instituto de Química, Universidad Nacional Autónoma de México, Circuito Exterior.Cd. Universitaria Coyoacán, México D.F. 04510, México*
[d] *Facultad de Química, Universidad Nacional Autónoma de México, Circuito Exterior Cd. Universitaria Coyoacán, México D.F. 04510, México*

Abstract

The synthesis, characterization, crystal structures and catalytic activity of four new 1,3-bis(aryl)triazenide(*p*-cymene)ruthenium(II) complexes bearing methoxycarbonyl (**5**), hydroxymethyl (**6**), acethylphenyl (**7**) in the *ortho* position, and methyl in the *para* position (**8**) of the bis(aryl)triazenide ligand are reported. These complexes were used as catalysts in the transfer hydrogenation reactions of ketones and alkenenone with good to excellent yields of the corresponding alcohol. Remarkable differences in yields were obtained with those complexes with *ortho* substituents on the aryl group of the triazenide ligand (**5-7**) compared to that without *ortho* substituent (**8**). Good selectivity was also observed in the reduction of the alkenone towards the carbonyl group.

1. Introduction

For the last decades, coordination and organometallic chemistry have focused on the design and development of alternative ligands to stabilize metal complexes and control their reactivity. With this in mind we have directed our attention to ligands of the type 1,3-bis(aryl)triazenide, since they exhibit a variety of bonding modes with distinct properties [1,2]. Triazenide ligands can act as monodentate binding through a terminal [3,4] or central nitrogen [5,6] as bidentate to form a chelate [7,8], bidentate bridging two metal centers [9,10] or tricoordinate bridges [11] and tetracoordinate bridges [12] (Fig. 1).

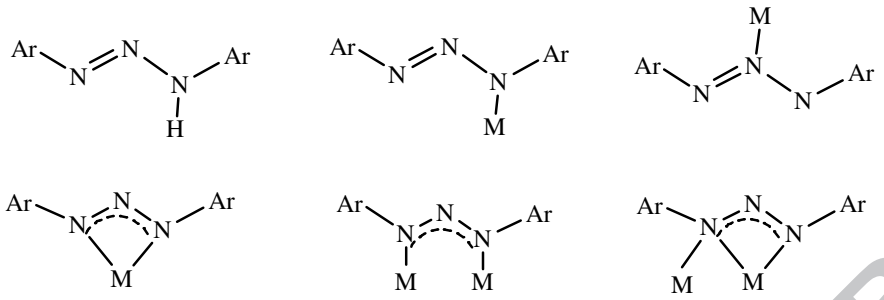

Figure 1. A generic triazene and binding modes of triazenide ligands.

It can be expected that incorporation of donor groups at the *ortho* position of the 1,3-bis(aryl)triazenide would produce a markedly different coordination chemistry. Thus we have turned our attention to the application of 1,3-bis(aryl)triazenide ligands bearing Lewis basic *ortho* substituents [13-17], expecting that they influence the electronic and steric properties of their complexes, which in turn determine their catalytic activity.

On the other hand, *p*-cymene complexes of ruthenium with 1,3-bis(aryl)triazenide as supporting ligands are attracting current interest from the point of view of their synthesis and structure, as catalysts in hydrogenation of enones, and anticancer activity. In this context, Strähle and coworkers reported the synthesis and structure of the first complex of this type, [RuCl(η^2-1,3-$ClC_6H_4NNNC_6H_4Cl$)(η^6-*p*-cymene)] [18]. More recently, Albertin and coworkers, reported neutral complexes [RuCl(η^2-1,3-ArNNNAr)(η^6-*p*-cymene)], their structures and catalytic activity on hydrogenation of 2-cyclohexen-1-one and cynamaldehyde under H_2 pressure [19]. Košmrlj, Osmak and coworkers have reported a series of 1,3-bis(aryl)triazenide(*p*-cymene)ruthenium(II) complexes with a high *in vitro* anticancer activity as the first study on the biological properties of this class of complexes [20].

Here we report on the synthesis of four complexes of formula [RuCl(η^2-1,3-ArNNNAr)(η^6-*p*-cymene)] (Ar = *o*-$COOCH_3$, *o*-CH_2OH, *o*-$COCH_3$ and *p*-tolyl) and their X-ray molecular structures. The catalytic activity of these complexes in the transfer hydrogenation of ketones and enones was evaluated with excellent results.

2. Experimental Section

2.1. General comments

All synthetic work was carried out in air or under argon using standard Schlenk techniques or an inert atmosphere dry-box where indicated. All solvents were dried over appropriate drying agents. $RuCl_3 \bullet 3H_2O$ (Aldrich) and other reagents are commercially available and were used as received. $[RuCl_2(p\text{-cymene})]_2$ [21], 1,3-bis[2´-(methoxycarbonyl)phenyl]triazene (**1**) [22], {1-[2-(hydroxymethyl)phenyl]-3-[4-methylphenyl]}triazene (**2**) [17] and 1,3-bis(4'-methylphenyl)triazene (**4**) [23] were synthesized according to previously reported procedures. NMR spectra were recorded at 400 MHz with Bruker Avance III spectrometer at 30 °C unless otherwise specified. ^1H and ^{13}C NMR chemical shifts are reported in ppm referenced to residual solvent resonances (^1H NMR: 7.16 for C_6HD_5 in C_6D_6, 1.94 for CHD_2CN in CD_3CN, 2.05 for acetone-d_5 in acetone-d_6. ^{13}C NMR: 128.39, 1.39, and 29.92 for benzene-d_6, acetonitrile-d_3 and acetone-d_6, respectively). Coupling constants *J* are given in Hertz (Hz). IR spectra were recorded on a Perkin-Elmer FT-IR 1605 spectrophotometer. Melting points were measured in an Electrothermal GAC 88629 apparatus. High Resolution Mass Spectrometry (HRMS) data were obtained in a micrOTOF-Q III MS instrument with electrospray ionization using sodium formate as calibrant.

2.2. Ligands

2.2.1. 1,3-bis(2´-acethylphenyl)triazene (**3**)

At −5 °C, 2'-aminoacetophenone (2.22 g, 16.4 mmol) was mixed with an excess of isoamyl nitrite (1.92 g, 16.4 mmol) in toluene (18 mL), and vigorously stirred for 24 h. The reaction mixture was dried over $MgSO_4$. The product was purified by crystallization at −5 °C from a 9:1 toluene/hexane mixture to obtain an amber crystalline solid (1.55 g, 5.53 mmol, 67%). MP = 118-120 °C; IR (ATR): 3188, 3000, 2950, 1665, 1648, 1576, 1505, 1462, 1429, 1255, 1230, 1186, 1161, 758 cm^{-1}. ^1H NMR [CD_3CN, 400 MHz]: δ 13.15 (s, 1H, NH), 8.04 (dd, *J* = 8.0, 1.2 Hz, 1H, Ar_{B6}), 7.90 (d, *J* = 8.4 Hz, 1H, Ar_{B3}), 7.64 (d, *J* = 8.0 Hz, 1H, Ar_{A3}), 7.61 (td, *J* = 8.0, 1.6 Hz, 1H, Ar_{B4}), 7.55 (td, *J* = 8.0, 1.6 Hz, 1H, Ar_{A4}), 7.52 (d, *J* = 8.0 Hz, 1H, Ar_{A6}), 7.39 (td, *J* = 7.0, 1.2 Hz, 1H, Ar_{A5}), 7.17 (td, *J* = 7.8, 1.2 Hz, 1H, Ar_{B5}), 2.66 (s, 3H, O=C-$CH_{3(B1)}$), 2.51 (s, 3H, O=C-$CH_{3(A1)}$). ^{13}C {^1H} NMR [CD_3CN, 100 MHz]: δ 203.6 (C_{B7}=O), 203.2 (C_{A7}=O), 148.3 (C_{A2}-N), 143.7 (C_{B2}-N), 137.4 (C_{A1}-C=O), 136.1 (C_{B4}-H), 133.4 (C_{B6}-H), 132.4 (C_{A4}-H), 128.9 (C_{A6}-H), 128.8 (C_{A5}-H), 122.9 (C_{B5}-H), 120.8 (C_{A3}-H), 120.3 (C_{B1}-C=O), 115.2 (C_{B3}-H), 32.4 (C_{A8}-C=O), 28.8 (C_{B8}-C=O). HRMS (ESI-TOF) m/z: $[M + Na]^+$ Calcd for $C_{16}H_{15}N_3O_2Na$ 304.1056; Found 304.1063.

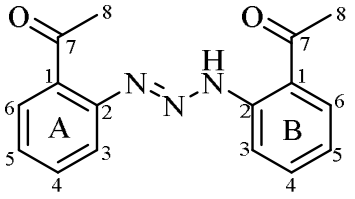

2.3. Synthesis of complexes

2.3.1. [Ru{1,3-bis[2´-(methoxycarbonyl)phenyl]triazenide}(Cl)(*p*-cymene)] (**5**)

1,3-bis[2´-(methoxycarbonyl)phenyl]triazene (**1**) (62.6 mg, 0.2 mmol) was dissolved in CH_2Cl_2 (5 mL) and triethylamine (56.8 µL, 0.4 mmol) was added with stirring. Then, a

solution of $[RuCl_2(p\text{-cymene})]_2$ (61.2 mg, 0.1 mmol) in CH_2Cl_2 (5 mL) was slowly added and the mixture stirred for 24 h at room temperature. A dark orange solution was formed, which was filtered through an alumina column. The solvent was removed under reduced pressure to obtain a red solid. Recrystallization by vapor diffusion of hexane into a concentrated solution of the product in THF at room temperature gave red crystals, suitable for X-ray diffraction analysis (85.6 mg, 0.15 mmol, 73%). MP = 136-140 °C. IR(ATR): 3062, 2962, 1720, 1593, 1432, 1382, 1294, 1247, 1082, 767, 721 cm^{-1}. ^1H NMR [C_6D_6, 400 MHz]: δ 7.50 (dd, J = 7.6, 1.6 Hz, 2H, Ar_{A3}), 7.45 (dd, J = 8.0, 0.8 Hz, 2H, Ar_{A6}), 7.12 (td, J = 8.0, 1.6 Hz, 2H, Ar_{A4}), 6.80 (td, J = 7.6, 0.8 Hz, 2H, Ar_{A5}), 5.16 (d, J = 6.0 Hz, 2H, p-$Cym_{C2,6}$), 4.83 (d, J = 6.0 Hz, 2H, p-$Cym_{C3,5}$), 3.69 (s, 6H, $-OCH_{3(A8)}$), 2.68 (sept, J = 6.8 Hz, 1H, p-Cym-$C\underline{H}_{(C7)}$-$(CH_3)_2$), 1.92 (s, 3H, p-Cym-$C\underline{H}_{3(C10)}$), 1.01 (d, J = 6.8 Hz, 6H, CH-$C\underline{H}_{3(C8,9)}$). ^{13}C {^1H} NMR [C_6D_6, 100 MHz]: δ 169.1 (C_{A7}=O), 147.2 ($\underline{C}_{A2}$-$COOCH_3$), 131.6 (C_{A4}-H), 130.0 (C_{A3}-H), 125.0 (C_{A1}-N), 125.0 (C_{A5}-H), 124.5 (C_{A6}-H), 103.2 ($\underline{C}_{C1}$-$CH(CH_3)_2$), 99.3 ($\underline{C}_{C4}$-CH_3), 82.0 ($C_{C2,6}$-H), 80.4 ($C_{C3,5}$-H), 52.4 ($-OCH_{3(A8)}$), 31.8 (p-Cym-$\underline{C}H_{(C7)}$-$(CH_3)_2$), 22.8 (CH-$\underline{C}H_{3(C8,9)}$), 19.2 (Ar-$\underline{C}H_{3(C10)}$). HRMS (ESI-TOF) m/z: $[M + Na]^+$ Calcd for $C_{26}H_{28}ClN_30_4RuNa$ 606.0708; Found 606.0706. Anal. Calcd for $C_{26}H_{28}ClN_3O_4Ru$ (583.04): C, 53.56; H, 4.84; N, 7.21. Found: C, 53.35; H, 4.77; N, 6.93.

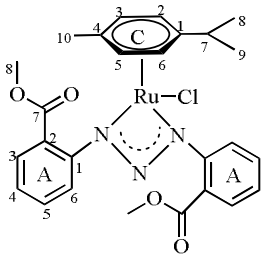

2.3.2. [Ru{1-[2-(hydroxymethyl)phenyl]-3-[4-methylphenyl]triazene}(Cl)(p-cymene)] (**6**)

Complex **6** was prepared in the same manner as complex **5**, using triazene **2** to obtain a solid which was crystallized by slow diffusion of hexane in a concentrated solution of the product in benzene at room temperature to give red crystals suitable for X-ray diffraction analysis (0.078 g, 0.12 mmol, 74%). MP = 71-74 °C. IR(ATR): 3395, 3026, 2962, 1597, 1503, 1448, 1273, 1032, 814, 755, 637 cm^{-1}. ^{1}H NMR [C_6D_6, 400 MHz]: δ 7.44 (d, *J* = 7.2 Hz, 1H, Ar_{A6}), 7.40 (d, *J* = 7.2 Hz, 1H, Ar_{A3}), 7.36 (d, *J* = 8.0 Hz, 2H, $Ar_{B2,6}$), 7.24 (t, *J* = 7.2 Hz, 1H, Ar_{A5}), 7.03 (t, 3H, Ar_{A4}), 7.01 (d, *J* = 8.0 Hz, 2H, $Ar_{B3,5}$), 5.02 (d, *J* = 5.6 Hz, 1H, *p*-Cym_{C6}), 4.90 (m, 1H, *p*-Cym_{C2}), 4.90 (m, 2H, Ar-C$\underline{H}_{2(A7)}$-OH), 4.62 (d, *J* = 5.6 Hz, 1H, *p*-Cym_{C3}), 4.58 (d, *J* = 5.6 Hz, 1H, *p*-Cym_{C5}), 3.40 (s, 1H, -O$\underline{H}_{A8}$), 2.32 (sept, *J* = 6.8 Hz, 1H, *p*-Cym-C$\underline{H}_{(C7)}$-$(CH_3)_2$), 2.14 (s, 3H, Ar-C$\underline{H}_{3(B7)}$), 1.91 (s, 3H, Ar-C$\underline{H}_{3(C2)}$), 0.86 (d, *J* = 6.8 Hz, 3H, CH-C$\underline{H}_{3(C8)}$), 0.84 (d, *J* = 6.8 Hz, 3H, CH-C$\underline{H}_{3(C9)}$). ^{1}H NMR [CD_3CN, 400 MHz]: δ 7.42 (dd, *J* = 7.6, 1.2 Hz, 1H, Ar), 7.33 (ddd, *J* = 7.2, 1.6 Hz, 1H, Ar), 7.25 (dd, *J* = 8, 1.2 Hz, 1H, Ar), 7.16 (m, 5H, Ar), 5.89 (d, *J* = 5.2 Hz, 1H, *p*-Cym), 5.77 (d, *J* = 6.8 Hz, 1H, *p*-Cym), 5.42 (d, *J* = 6.4 Hz, 2H, *p*-Cym), 4.68 (dd, $^{2}J_{HH}$ = 13.6, $^{3}J_{HH}$ = 7.2 Hz, 1H, Ar-C$\underline{H}_2$-OH), 4.58 (dd, $^{2}J_{HH}$ = 13.6, $^{3}J_{HH}$ = 6 Hz, 1H, Ar-C$\underline{H}_2$-OH), 3.30 (dd, *J* = 7.2, 6.4 Hz, 1H, O$\underline{H}$), 2.67 (sept, *J* = 7.2 Hz, 1H, *p*-Cym-C$\underline{H}$-$(CH_3)_2$), 2.33 (s, 3H, Ar-C$\underline{H}_3$), 2.23 (s, 3H, Ar-C$\underline{H}_3$), 1.18 (d, *J* = 6.9 Hz, 3H, CH-C$\underline{H}_3$), 1.16 (d, *J* = 6.9 Hz, 3H, CH-C$\underline{H}_3$). ^{13}C {^{1}H} NMR [C_6D_6, 100 MHz]: δ 147.2 (C_{A1}-N), 145.6 (C_{B1}-N), 134.1 ($\underline{C}_{B4}$-CH_3), 132.9 ($\underline{C}_{A2}$-CH_2OH), 131.1 (C_{A3}-H), 129.8 ($C_{B3,5}$-H), 128.4 (C_{A5}-H), 125.1 (C_{A4}-H), 122.5 (C_{A6}-H), 117.7 ($C_{B2,6}$-H), 102.5 ($\underline{C}_{C1}$-$CH(CH_3)_2$), 101.7 ($\underline{C}_{C4}$-CH_3), 81.7 (C_{C2}-H), 81.1 (C_{C6}-H), 79.9 (C_{C3}-H), 79.1 (C_{C5}-H), 62.8 (Ar-$\underline{C}H_{2(A7)}$-OH), 31.7 (*p*-Cym-$\underline{C}H_{(C7)}$-$(CH_3)_2$), 22.5 (CH-$\underline{C}H_{3(C8)}$), 22.4 (CH-$\underline{C}H_{3(C9)}$), 21.0 (Ar-$\underline{C}H_{3(B7)}$), 19.0 (*p*-Cym-$\underline{C}H_{3(C10)}$). HRMS (ESI-TOF) m/z: $[M + Na]^+$ Calcd for $C_{24}H_{28}ClN_3ORuNa$ 534.0860; Found 534.0861.

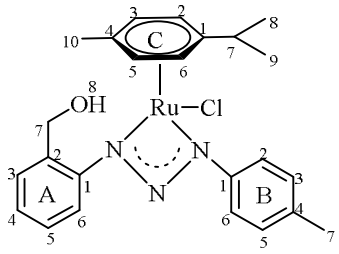

2.3.3. [Ru{1,3-bis(2´-acethylphenyl)triazenide}(Cl)(*p*-cymene)] (**7**)

Complex **7** was prepared in the same manner as complex **5**, using triazene **3** to obtain a solid which was crystallized by slow evaporation of a concentrated solution of the product in THF at room temperature to give amber crystals suitable for X-ray diffraction analysis (83.2 mg, 0.15 mmol, 76%). MP = 126-131 °C. IR(ATR): 3060, 2964, 1699, 1593, 1432, 1382, 1294, 1247, 1082, 767, 721 cm^{-1}. ^{1}H NMR [acetone-d_6,, 400 MHz]: δ 7.42 (td, J = 6.8, 1.6 Hz, 2H, Ar_{A5}), 7.36 (dd, J = 8.0, 1.2 Hz, 2H, Ar_{A6}), 7.23 (dd, J = 7.6, 1.6 Hz, 2H, Ar_{A3}), 7.17 (td, J = 6.8, 1.6 Hz, 2H, Ar_{A4}), 5.99 (d, J = 6.4 Hz, 2H, *p*-$Cym_{C2,6}$), 5.67 (d, J = 6.4 Hz, 2H, *p*-$Cym_{C3,5}$), 2.90 (sept, J = 6.8 Hz, 1H, *p*-Cym-C$\underline{H}_{(C7)}$-$(CH_3)_2$), 2.30 (s, 3H, *p*-Cym-C$\underline{H}_{3(C10)}$), 2.30 (s, 6H, O=C-$CH_{3(A8)}$), 1.29 (d, J = 6.8 Hz, 6H, CH-C$\underline{H}_{3(C8,9)}$). ^{13}C {^{1}H} NMR [acetone-d_6, 100 MHz]: δ 202.8 (C_{A7}=O), 145.5 (C_{A1}-N), 133.7 ($\underline{C}_{A2}$-$COCH_3$), 131.3 (C_{A5}-H), 128.3 (C_{A3}-N), 125.5 (C_{A4}-H), 124.0 (C_{A6}-H), 104.8 ($\underline{C}_{C1}$-$CH(CH_3)_2$), 101.5 ($\underline{C}_{C4}$-CH_3), 82.9 ($C_{C2,6}$-H), 81.4 ($C_{C3,5}$-H), 32.6 (*p*-Cym-C$\underline{H}_{(C7)}$-$(CH_3)_2$), 30.9 (O=C-C$\underline{H}_{3(A8)}$), 23.0 (CH-C$\underline{H}_{3(C8,9)}$), 19.5 (Ar-C$\underline{H}_{3(C10)}$). HRMS (ESI-TOF) m/z: $[M + Na]^+$ Calcd for $C_{26}H_{28}ClN_3O_2RuNa$ 574.0809; Found 574.0797. Anal. Calcd for $C_{26}H_{28}ClN_3O_2Ru$ (551.04): C, 56.67; H, 5.12; N, 7.63. Found: C, 56.49; H, 5.04; N, 7.31.

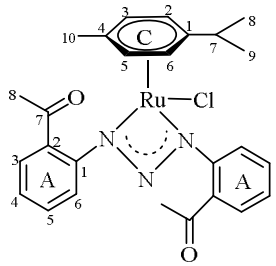

2.3.4. [Ru{1,3-bis(4´-methylphenyl)triazenide}(Cl)(*p*-cymene)] (**8**)

Complex **8** was prepared in the same manner as complex **5**, using triazene **4** to obtain a solid which was crystallized by slow diffusion of pentane in a concentrated solution of the product in CH_2Cl_2 at room temperature to give red crystals suitable for X-ray diffraction analysis (0.064 g, 0.13 mmol, 80%). MP = 187-189 °C. IR(ATR): 3026, 2963, 2914, 1603, 1466, 1370, 1276, 1106, 820, 660 cm^{-1}. ^1H NMR [acetone-d_6, 400 MHz]: δ 7.24 (d, J = 8.4 Hz, 4H, $Ar_{A2,6}$), 7.10 (d, J = 8.4, Hz, 4H, $Ar_{A3,5}$), 6.02 (d, J = 6.4 Hz, 2H, *p*-$Cym_{C2,6}$), 5.56 (d, J = 6.4 Hz, 2H, *p*-$Cym_{C3,5}$), 2.78 (sept, J = 6.8 Hz, 1H, *p*-Cym-C$\underline{H}_{(C7)}$-$(CH_3)_2$), 2.29 (s, 6H, Ar-$CH_{3\ (A7)}$), 2.26 (s, 3H, *p*-Cym-$CH_{3(C10)}$), 1.23 (d, J = 6.8 Hz, 6H, CH-C$\underline{H}_{3(C8,9)}$). ^{13}C {^1H} NMR [acetone-d_6, 100 MHz]: δ 146.3 ($\underline{C}_{A4}$-CH_3), 133.9 (C_{A1}-N), 130.0 ($C_{A3,5}$-H), 117.8 ($C_{A2,6}$-H), 103.0 ($\underline{C}_{C4}$-CH_3), 102.9 ($\underline{C}_{C1}$-$CH(CH_3)_2$), 82.4 ($C_{C2,6}$-H), 80.0 ($C_{C3,5}$-H), 32.6 (*p*-Cym-$\underline{C}H_{(C7)}$-$(CH_3)_2$), 22.8 (CH-$\underline{C}H_{3(C8,9)}$), 20.9 (Ar-$\underline{C}H_{3(A7)}$), 19.2 (Ar-$\underline{C}H_{3(C10)}$). HRMS (ESI-TOF) m/z: $[M + Na]^+$ Calcd for $C_{24}H_{28}ClN_3RuNa$ 518.0911; Found 518.0917.

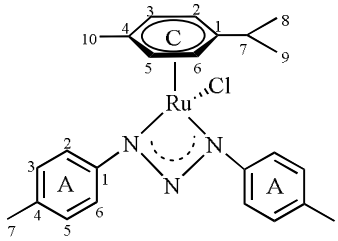

2.4 X-ray crystallography

The crystals of compounds **5** and **7** were mounted on a glass fiber at room temperature, and then placed on a Bruker SMART APEX CCD-based X-ray diffractometer system equipped with a Mo-target X-ray tube (λ = 0.71073Å). The detector was placed at a distance of 5.0 cm from the crystals; in all cases, decay was negligible. A total of 1800

frames were collected with a scan width of 0.3 in x and an exposure time of 10 s/frame. The frames were integrated with the Bruker SAINT Software package using a narrow-frame integration algorithm. Systematic absences and intensity statistics were used in space group determination.

The structures were solved using direct methods using SHELXS-2014/7 program [24]. Anisotropic structure refinements were achieved using full matrix, least-squares technique on all non-hydrogen atoms. All hydrogen atoms were placed in idealized positions, based on hybridization, with isotropic thermal parameters fixed at 1.2 times the value of the attached atom. Structure refinements were performed using SHELXL-2014/7 [24].

Isopropyl and phenyl group atoms on compound **5** are disordered, and were refined anisotropically, in two major contributors, using a variable site occupational factor (SOF). The ratio of SOF was 0.56/0.47 for C24, C25 of isopropyl atoms and 0.63/0.37 for C9-C12.

Crystals of compounds **3, 6** and **8** were mounted under paratone on glass fiber; then, the crystal was immediately cooled at 130 K using a Cryojet cryostream (Oxford Cryosystems device). Diffraction data were collected on an Oxford Diffraction Gemini diffractometer with a CCD-Atlas area detector using a radiation source graphite monochromator, $\lambda_{MoK\alpha}$ = 0.71073 Å. CrysAlisPro and CrysAlis RED software packages [25] were used for data collection and data integration. Collected data were corrected for absorbance using analytical numeric absorption correction [26] with a multifaceted crystal model based on expressions upon the Laue symmetry using equivalent reflections.

Structure solution and refinement were carried out with SHELX-2014 [27] and SHELXL-2014 software, and ORTEP-3 for Windows [28] was used for molecular

graphics. WinGX [29] software was used to prepare material for publication. Full-matrix least-squares refinement was carried out by minimizing $(Fo^2 - Fc^2)^2$. All non-hydrogen atoms were refined anisotropically.

The H atom of the amine (H–N) and hydroxyl groups (H–O) group were located in the difference map and refined isotropically with U_{iso}(H) = 1.2 U_{eq} (N) and 1.5 U_{eq} (N). H atoms attached to C atoms were placed in geometrically idealized positions and refined as riding on their parent atoms, with C–H = 0.95–1.00 Å and U_{iso} (H) = 1.2U_{eq}(C) for aromatic, methylene and methyne groups, and 1.5 U_{eq}(C) for methyl group.

2.5 General procedure for transfer hydrogenation studies monitored by ^{1}H NMR.

All measurements were made on a Bruker 400 spectrometer operating at 400 MHz. Inside a nitrogen glovebox, acetophenone (6×10^{-5} mol), 1,3,5-trimethylbenzene (2 μL) as internal standard and 0.6 mL of 2-propanol-d_8 were transferred into a J-Young NMR tube. The tube was closed in order to avoid air contamination, and a ^{1}H NMR spectrum was recorded. Next, the tube was brought back into the glovebox and the ruthenium precatalyst (1.2×10^{-6} mol) and KOH (6×10^{-6} mol) added. Outside of the glovebox the tube was placed in an oil bath at 70 °C. At the desired sampling time, the tube was taken out of the oil bath, and a ^{1}H NMR spectrum was recorded. Percent conversions were determined by comparing the integration of the aromatic protons at the *ortho* position of the alcohol with the aromatic protons at the *ortho* position of the acetophenone. The value of the integral for the singlet due to the aromatic protons of 1,3,5-trimethylbenzene (internal standard) was set equal to 10 units in each case.

2.6 General protocol for catalytic transfer hydrogenation monitored by Gas Chromatography-Mass Spectrometry (GC-MS).

Complex **6** (1.2×10^{-6} mol), 6-methyl-5-hepten-2-one (6×10^{-5} mol) and 2-propanol (0.6 mL) were transferred into a 2 mL vial. The resulting solution was heated at 70 ºC

and the reaction progress was monitored by GC-MS analysis in order to calculate the conversion of the substrate 6-methyl-5-hepten-2-one. After 11 h of reaction, an aliquot of 0.2 mL was taken and filtered through a short pad of silica gel and diluted to 1.0 mL with 2-propanol.

The analytical GC/MS system used was an Agilent 7890A GC coupled to 5975C Mass detector Agilent Technologies, equipped with a HP-5MS capillary column (30 m × 0.25 mm × 0.25 micron) Agilent Technologies, Inc. An Agilent Technologies 7693 auto sampler was used to inject 1 μL of a solution sample. The ionization energy was 70 eV with a mass range of 30 to 800 m/z. The initial temperature of the column was set at 80 ºC, held for 2 min, and then a ramp of 10 ºC/min to 250 ºC. The temperature of the injector was set at 250 ºC and the detector at 230 ºC. The flow rate of the carrier gas (Helium) was 1.0 mL/min injected with a gas dilution of 1:50. Identification of the individual components was based on comparison with the mass spectra library (NIST98).

3. Results and discussion

3.1. Synthesis and general characterization

3.1.1. Ligands

Triazenes **1** [22], **2** [17] and **4** [23] were synthesized according to previously reported procedures. Triazene **3** was synthesized following modified literature procedures in a one-step reaction by coupling of *o*-aminoacetophenone, using isoamyl nitrite in toluene [30].

The IR spectrum of triazene **3** shows bands at 3188 cm^{-1} for the N–H group and 1576 cm^{-1} for the N_3 system. The C=O groups appear at 1665 and 1648 cm^{-1}, indicating the asymmetry due to the N=N–N system. The ^1H NMR spectrum of the triazene **3** shows a broad singlet at 13.10 ppm assigned to the triazene N–H group. In the region

8.05-7.15 ppm four doublets and four triplets which integrate for eight hydrogen atoms on two *ortho* disustituted non-equivalent aromatic rings. The signal of the acetyl groups (-$COCH_3$) appears as two singlets at 2.66 and 2.51 ppm, which integrate for the six hydrogens. The ^{13}C NMR spectrum shows 12 signals for the carbon atoms in the aromatic region, two carbonyl signals at 203.6 and 203.2, and two methyl signals at 32.4 and 28.8 ppm for the two *ortho*-acetyl groups. This behavior is a consequence of an intramolecular hydrogen bond [C(1)=O(1)---HN(1)] in solution, where the carbonyl group involved in the hydrogen bond is shifted downfield (203.6 ppm) due to electron density donation. EIMS confirmed the molecular weight (281 uma) for triazene **3** and its analysis by HRMS gives a peak with *m/z* = 304.1063which is consistent with the formation of adduct $[M + Na]^+$ in the gas phase.

3.1.2. Ruthenium Complexes

Reaction of 1,3-bis(aryl)triazene ligand precursors (**1**-**4**) with half equivalent of $[RuCl(p\text{-cymene})(\mu\text{-}Cl)]_2$ in dichloromethane at room temperature and in presence of trimethylamine, resulted in the formation of new monomeric [RuCl(η^2-1,3-ArNNNAr)(η^6-*p*-cymene)] complexes (**5-8**) (Equation 1).

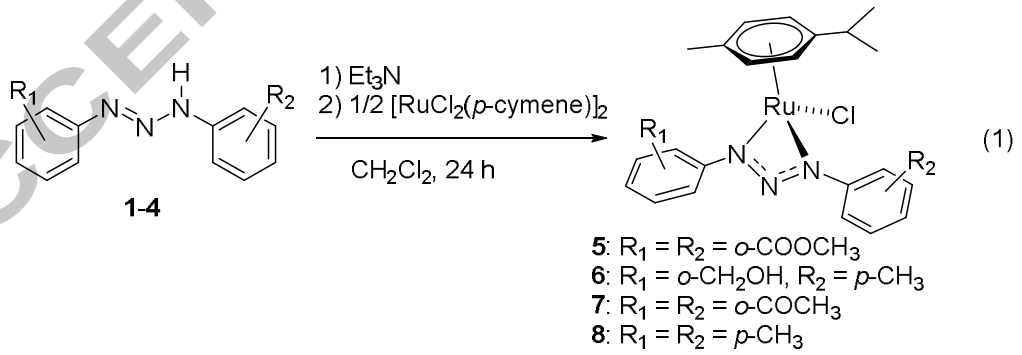

(1)

Complexes **5**-**8** were isolated as stable yellow or red solids. Their formulation is supported by analytical and spectroscopic data (IR, HRMS and NMR spectra), and X-ray crystal structure determination.

In the ^{1}H NMR spectra of complexes **5**, **7** and **8**, the *p*-cymene aromatic protons are observed as two doublets in the range of 6.0-4.8 ppm, while the isopropyl methyl protons appear as doublets in the range of 1.30-1.02 ppm. These results are in agreement with the (*p*-cymene)Ru(triazenide)(L) complexes previously reported [18-20]. In contrast, in complex **6** the *p*-cymene aromatic protons are observed as four doublets (one of them is overlapped with the methylene signal) and the isopropyl methyl protons are also inequivalent, appearing as two doublets at 0.86 and 0.84 ppm. It has been suggested that this is a consequence of the chirality of the Ru center due to the coordination of the asymmetric triazenide ligand from **2**. This behavior has been observed in related asymmetric (*p*-cymene)Ru(N^N) complexes [36-38]. On the other hand, all the complexes show a septet in the range of 2.90-2.32 ppm for the isopropyl CH protons. The same behavior can be seen in the ^{13}C NMR spectra. For example, signals for the isopropyl methyl carbons appear in the range of 23-22 ppm in complexes **5**, **7** and **8**, while in complex **6** two signals at 22.5 and 22.4 ppm are observed.

The aromatic rings in the 1,3-diaryltriazenide ligands give signals and integration for equivalent *ortho*-disubstituted aromatic rings (**5** and **7**), *para*-disubstituted (**8**) and the presence of both systems in complex **6**. Additional equivalent methyl signals are observed as singlets at 2.30 and 2.29 ppm for complexes **7** and **8**, respectively. The equivalent methoxy groups of complex **5** are observed as a singlet at 3.64 ppm. Interestingly, when complex **6** is analyzed in C_6D_6 the signal of the methylene group (-C$\underline{H}_2$OH) is overlapped with the resonance of one *p*-cymene hydrogen *ortho* to the isopropyl group [H(16)], and the O$\underline{H}$ appears as a broad multiplet. In contrast, if **6** is analyzed in CD_3CN the hydrogens of the methylene becomes diastereotopic and are observed as a set of two doublet of doublets at 4.68 and 4.58 ppm with $^{2}J_{HH}$ = 13.6, $^{3}J_{HH}$ = 7.2 Hz and $^{2}J_{HH}$ = 13.6, $^{3}J_{HH}$ = 6 Hz, respectively.

Moreover, the OH hydrogen appears as a doublet of doublets at 3.30 ppm with $^{3}J_{HH}$ = 7.2 and, $^{3}J_{HH}$ = 6.4 Hz. In the ^{13}C NMR spectra it is of relevance the carbonyl signals of the *ortho*-methoxycarbonyl (169.1 ppm) and *ortho*-acetyl (202.8 ppm) groups in complexes **5** and **7**, respectively; in both cases the carbonyl signals are equivalent, unlike those in the free triazene **3**. The methylene carbon in the *ortho*-hydroxymethylene group in complex **6** appears at 62.8 ppm. The NMR assignments were confirmed by gCOSY, gHSQC and gHMBC experiments (see Supporting Information). Complexes **5**-**8** were analyzed by HRMS (ESI-TOF) and their spectra showed the formation of adducts of the type $[M + Na]^{+}$, which may be a consequence of using sodium formate as calibrant.

3.2. Description of the crystal structures

Amber crystals of triazene **3** suitable for X-ray diffraction were obtained from a toluene/hexane mixture. Compound **3** crystallized in the orthorhombic crystalline system with the space group P bca. The molecular structure of triazene **3** is shown in Figure 2 with bond distances and angles, while crystal data is given in Table 2. Triazene **3** adopts a *trans* configuration about the N=N double bond and is quasi planar with the dihedral angle between the two aromatic rings at 2.39°. The N(1)-N(2)=N(3) bond angle is 112.1(11)°. Also, the N(1)-N(2) and N(2)=N(3) bond distances are 1.333(15) Å and 1.259(16) Å, respectively, which indicates the presence of single and double bond. The bond distances and angles are in agreement with those reported for most related triazenes with *ortho*-substituents [31-35]. A distinct intramolecular hydrogen bond C(1)=O(1)---HN(1) is present, with a distance of 1.937(18) Å, while the C(6)=O(2) of the other *o*-acetyl group presents an interaction with the methyl hydrogen of the *o*-acetyl group of another molecule [C(6)=O(2)---H(16)'C(16)'] with a distance of 2.64(4) Å.

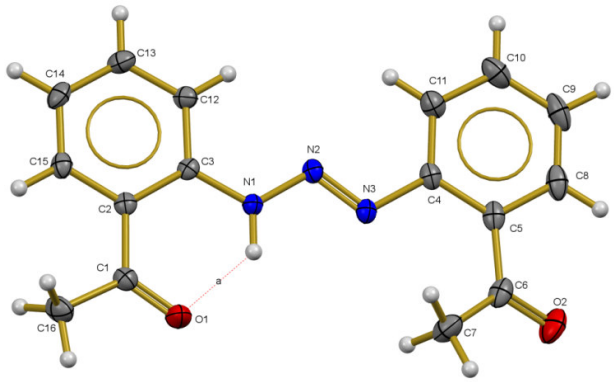

Figure 2. ORTEP picture of the molecular structure of compound **3** with thermal ellipsoids drawn at 50% probability level. Bond distances (Å): N(1)-N(2), 1.333(15); N(2)=N(3), 1.2590(16); N(1)-H(1D), 0.907(15); C(1)=O(1), 1.2245(18); C(6)=O(2), 1.2203(18). Bond angles (º): N(3)-N(2)-N(1), 112.09(11); N(2)-N(1)-H(1D), 119.9(13).

Crystals of the series of triazenide ruthenium complexes suitable for X-ray diffraction studies were obtained. Compounds **5**, **7** and **8** crystallized in the monoclinic crystalline system while **6** in the orthorhombic system, with different space groups (*Pn* for **5**, P21 21 21 for **6**, *P21/c* for **7** and *Cc* for **8**). Relevant crystallographic data are included in Table 1.

Table 1. Crystallographic data and refinement parameters for triazene **3**, and complexes **5**-**8**.

	3	**5**	**6**	**7**	**8**
Empirical formula	C_{16} H_{15} N_3 O_2	C_{26} H_{28} Cl N_3 O_4 Ru	C_{30} H_{34} Cl N_3 O Ru	C_{26} H_{28} Cl N_3 O_2 Ru	C_{24} H_{28} Cl N_3 Ru
fw	281.31	583.03	589.12	551.03	495.01
T(K)	173(2) K	298	173(2) K	298	130 (2) K
λ(Å)	0.71073 Å	0.71073	0.71073 Å	0.71073	0.71073 Å
Cryst syst	Orthorhombic	Monoclinic	Orthorhombic	Monoclinic	Monoclinic
Space group	P b c a	Pn	P 21 21 21	P 21/c	C c
Unit cell dimensions					
a(Å)	15.7858(11)	11.8640(12)	8.2430(4)	9.8554(9)	12.0989(8)
b(Å)	8.1374(5)	9.3238(9)	15.7074(8)	13.8618(13)	24.6543(13)
c(Å)	21.7015(13)	11.8597(12)	21.2161(10)	18.8855(18)	7.6486(5)
α(deg)	90	90	90	90	90
β(deg)	90	90.537(2)	90	101.289(2)º	109.497(8)
γ(deg)	90	90	90	90	90
V(Å^3)	2787.7(3)	1311.8(2)	2747.0(2)	2530.1(4)	2150.7(3)
Z	8	2	4	4	4
F(000)	1184	596	1216	1128	568

D_{Calc} (Mg/m^3)	1.341	1.476	1.424	1.447	1.437
$\mu(mm^{-1})$	0.091	0.735	0.695	0.752	0.869
R1(%)[a]	0.0844	0.0335	0.0411	0.0619	0.1241
wR2(%)[b]	0.1320	0.0796	0.0686	0.0752	0.1958

[a] $R1 = R||F_o| - |F_c||/R|F_o|$.
[b] $wR2 = [R[w(F_o^2 - F_c^2)^2]/R[w(F_o^2)^2]]^{1/2}$.

The ORTEP diagrams of complexes **5**-**8** are given in Figures 3-6 with selected bond lengths and angles. In all compounds the ruthenium atom is surrounded by the η^6-bonded *p*-cymene ring, a chelating η^2-triazenide ligand and one chloro ligand, attaining a pseudo-octahedral "three legged piano stool" geometry. The small-bite of the triazenide [N(1)-Ru-N(2), in the range of 58.84(12) to 59.28(8)] conditions the bond angles around the metal, but only those affecting this ligand, in such a way that the N-Ru-Cl angles are all close to the expected 90°. The Ru-N distances are in the range of 2.054(3)-2.132(3) Å, while the N-N bond lengths in the triazenide ligands are around 1.307 Å, a value which is between a single (N-N) and a double bond (N=N). The distances Ru-C and Ru-CT of the *p*-cymene ligand in the complexes have values between 2.151(4)-2.225(3) Å, and 1.6659(17)-1.676(2) Å, respectively. All these values are in the range found for the reported structures of (*p*-cymene)Ru-(triazenide) complexes [18-20] and are comparable to other Ru-triazenide complexes [39-45] (without the *p*-cymene ligand). Those values are also comparable with a *p*-cymene-Ru-triarylguanidinate complex [46] with an *o*-methoxy substituent of similar structure, the bite angle being slightly larger. As in the previously mentioned complex, **7** has a *syn* conformation with respect to the two *o*-acetyl substituent found as far away from the *p*-cymene ring, while **5** adopts an *anti*-conformation as a result of the steric hindrance exerted between the two *o*-methoxycarbonyl substituent. The lengths and angles of the *o*-substituent in complex **5** (*o*-methoxycarbonyl), **6** (*o*-hidroxymethyl), and **7** (*o*-acetyl) are in agreement with related structures [16], and in the case of **5** and **7**, this values are comparable to the *o*-substituent in triazene **1** [13] and **3**, respectively.

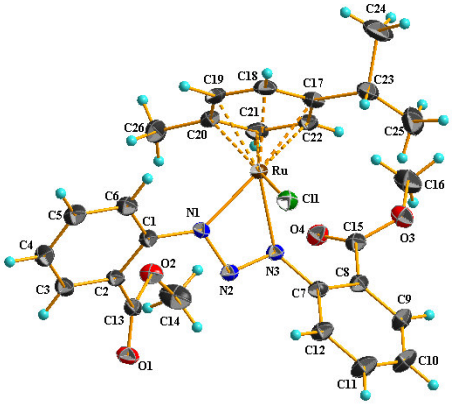

Figure 3. Structure of the asymmetric unit of **5** with thermal ellipsoids drawn at 20% probability level. Bond distances (Å): Ru-N1, 2.054(3); Ru-N3, 2.132(3); N(1)-N(2), 1.304(4); N(2)-N(3), 1.311(4); N(1)-C(1), 1.393(5); Ru-Cl1, 2.3927(11); Ru-CT, 1.670; Ru-C17, 2.226(6); Ru-C20, 2.176(5); C(13)=O(1), 1.211(5); C(15)=O(3), 1.192(5). Bond angles (°): N(1)-N(2)-N(3), 103.8(3); N1-Ru-N3, 58.85(12); Cl-Ru-N1, 85.04(10); Cl-Ru-N3, 84.59(10); O(2)-C(13)=O(1), 124.27.

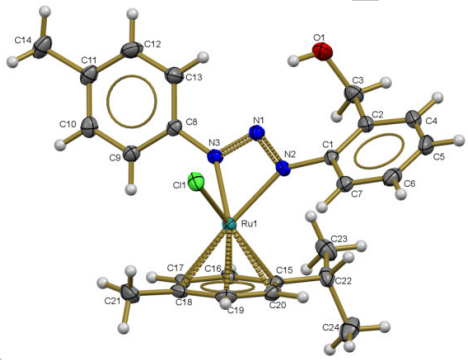

Figure 4. Structure of the asymmetric unit of **6** with thermal ellipsoids drawn at 50% probability level. Bond distances (Å): Ru-N1, 2.067(3); Ru-N3, 2.086(3); N(1)-N(2), 1.307(5); N(2)-N(3), 1.318(4); N(1)-C(1), 1.411(5); Ru-Cl, 2.3963(8); Ru-CT, 1.676; Ru-C17, 2.190(3); Ru-C20, 2.226(4); C(13)-O(1), 1.432(6); O(1)-H(1), 0.819(4). Bond angles (°): N(1)-N(2)-N(3), 102.9(3); N1-Ru-N3, 59.22(13); Cl-Ru-N1, 84.43(9); Cl-Ru-N3, 86.00(10); C(13)-O(1)-H(1), 109.6(6).

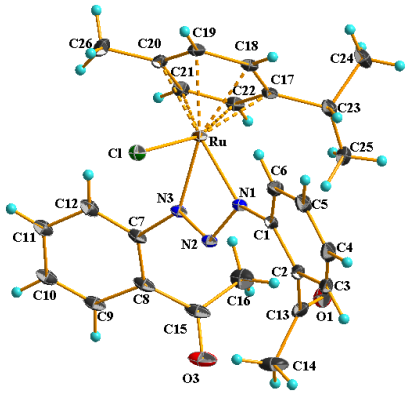

Figure 5. Structure of the asymmetric unit of **7** with thermal ellipsoids drawn at 10% probability level. Bond distances (Å): Ru-N1, 2.094(3); Ru-N3, 2.052(3); N(1)-N(2), 1.313(4); N(2)-N(3), 1.306(4); N(1)-C(1), 1.411(4); Ru-Cl1, 2.3890(11); Ru-CT, 1.666; Ru-C17, 2.185(4); Ru-C20, 2.190(4); C(13)=O(1), 1.208(5); C(15)=O(3), 1.211(5). Bond angles (°): N(1)-N(2)-N(3), 102.9(3); N1-Ru-N3, 59.16(12); Cl-Ru-N1, 85.63(10); Cl-Ru-N3, 85.89(8); C(14)-C(13)=O(1), 120.94(5); C(16)-C(15)=O(3), 120.9(6).

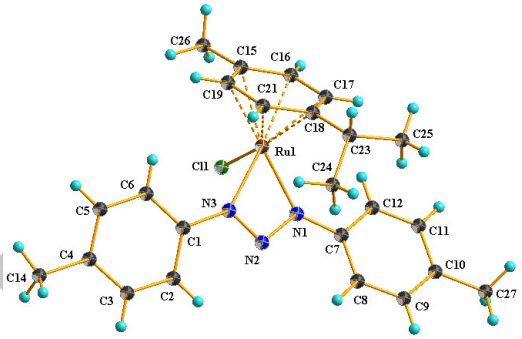

Figure 6. Structure of compound **8** with thermal ellipsoids drawn at 70% probability level. Bond distances (Å): Ru-N1, 2.057(4); Ru-N3, 2.083(4); N(1)-N(2), 1.323(5); N(2)-N(3), 1.301(5); N(1)-C(1), 1.395(5); Ru-Cl, 2.3936(7); Ru-CT, 1.676; Ru-C17, 2.207(5); Ru-C20, 2.228(5). Bond angles (°): N(1)-N(2)-N(3), 102.6(3); N1-Ru-N3, 59.29(14); Cl-Ru-N1, 85.93(11); Cl-Ru-N3, 85.22(10).

In all the complexes the crystal arrangement exhibits intermolecular C-H···Cl hydrogen bonds; complexes **5** and **7** exhibit intermolecular C-H···O hydrogen bonds; the crystal of complex **6** is stabilized by a benzene molecule, and complex **8** presents one π-π interaction between the phenyl rings of the triazenide ligand. For example in complex **7** the C-H···O interactions generate a 2D layer in the plane *ac* (Figure 7); these are formed by the interactions of the two C=O3 producing a bifurcated hydrogen bond [C8-H8···O3, 2.70 Å; C6-H6···O3, 2.61 Å] (Figure 7). The interactions C21-H21···Cl1

and C21-H21···$\pi_{C17-C22}$ complete the interactions leading to the formation of the 3D framework. The secondary interactions for the other complexes and triazene **3** are given in the Supporting Information, Figures S1-S3.

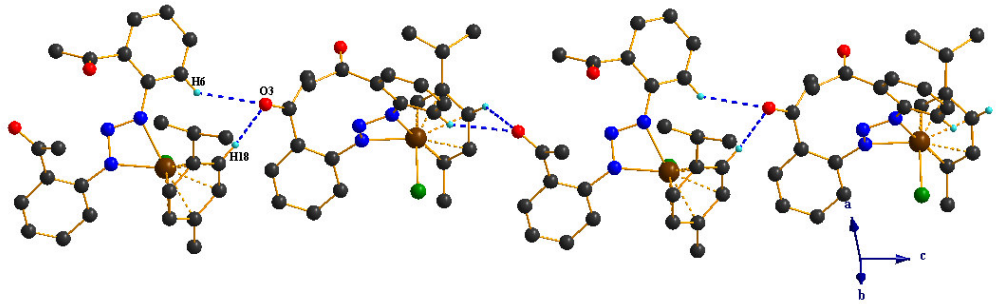

Figure 7. Representation of the bifurcated hydrogen bond in compound **7**. The hydrogen atoms not involved have been omitted for clarity.

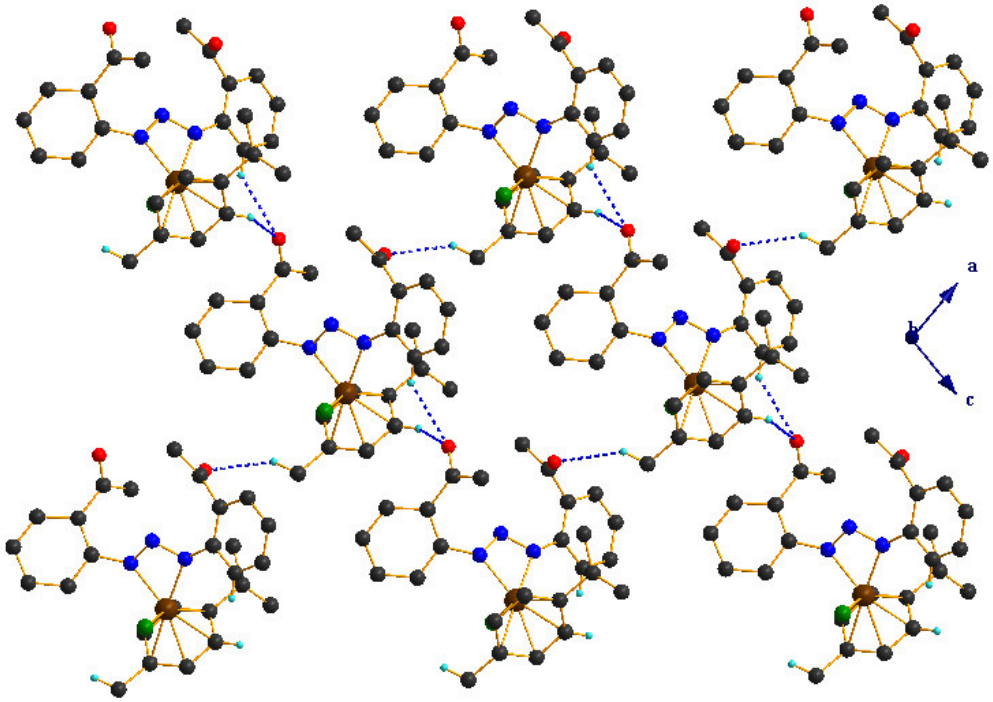

Figure 8. Representation of the 2D arrangement in compound **7**. Only the hydrogen atoms involved in the non covalent interactions have been drawn.

3.3 Transfer Hydrogenation Catalysis

Complexes **5**-**8** were tested in the catalytic reduction of acetophenone to 1-phenylethanol under the conditions showed in Equation 2.

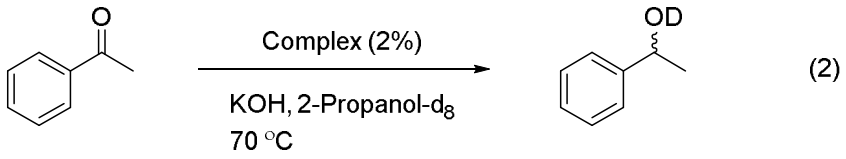

(2)

Table 1. Transfer hydrogenation of acetophenone using **5**-**8** as precatalysts.[a]

Catalyst	Entry	Substrate/Catalyst/KOH	Time (h)	Yield (%)[b]
5	1	100/2/10	12	94
5	2	100/2	24	86
6	3	100/2/10	5	96
6	4	100/2	24	42
7	5	100/2/10	12	78
8	6	100/2/10	12	9
8	7	100/2	24	15

[a]Reaction conditions: 2-propanol-d_8, 70 °C, with or without KOH as base. [b]Yields were determined by ^{1}H NMR.

The results of the catalytic evaluation are summarized in Table 1. After 12 h yields of 1-phenylethanol were 94 and 78% for **5** and **7**, respectively (entry 1 and 5). However, greater success was achieved by using **6** as precatalyst since a higher yield was obtained in less time (96% in 5 h, entry 3). Interestingly, complex **8**, lacking any *ortho*-substituent group at the triazenide ligand was almost ineffective in catalyzing transfer hydrogenation under the same conditions (9% after 12 h, entry 6). This result shows that the presence of an *ortho*-substituent with donating properties in the structure of the triazenide ligand enhance the activity of the catalysts. Moreover, it can be expected that the *ortho*-substituents can acts as a Lewis base accepting a proton or participating in a hydrogen bond as acceptor. With this assumption in mind, the ability of complexes (**5**, **6** and **8**) to hydrogenate acetophenone was also tested in absence of base. Interestingly, acetophenone was hydrogenated to 1-phenylethanol without using KOH, although the catalysis is not as fast when is compared with the system using KOH. Thus, **6** is the fastest catalyst but only when KOH is used. In the absence of base the

hydroximethylene substituent may be able to participate in hydrogen bonding and this may affect its activity (42% in 24 h) whereas **5** is the most active when no base is used (86% in 24 h). Further studies would be needed to explain the role of the *ortho*-substituent in the catalysis.

Under the same conditions of Equation 2, hydrogenation of benzophenone using **5** and **6** was also studied finding similar results, with yields of 94 and 98% after 12 and 5h, respectively. On the other hand, a more promising result was obtained when **6** was used to perform the chemoselective reduction of 6-methyl-5-hepten-2-one to 6-methyl-5-hepten-2-ol (Equation 3).

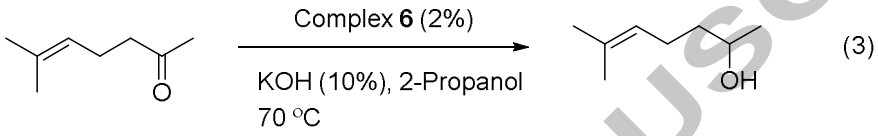

(3)

After 11 h of reaction, analysis of an aliquot by GC-MS showed a 96% yield of the unsaturated alcohol. This is an important result because there are several possibilities in the hydrogenation of this substrate because the C=C bond could also be hydrogenated or isomerized.

4. Conclusions

A series of four Ru(II) complexes of triazenide ligands (prepared from precursors **1**-**4**) have been synthesized and characterized by IR, HRMS, NMR and X ray diffraction. We have found that functional groups at the *ortho* position in triazenide ligands of complexes **5**-**7** do not participate as metal coordinating sites. However, comparing transfer hydrogenation using **5**-**7** and **8**, these *ortho* substituents clearly have an influence in the catalytic properties of complexes **5**-**7**. Complex **8**, although lacking *ortho* substituents on the bis(aryl)triazenide ligand showed some catalytic activity, probably due to the deprotonated triazene nitrogen, which may act as a Lewis base accepting one proton, thus forming a Noyori's type of hydride complex. However, we cannot discard the possibility that the *ortho* groups behave in the same manner. Therefore, catalysis may as well operate by a ligand assisted outer sphere

mechanism [47] analogous to that reported by Noyori for transfer hydrogenation. On the other hand, it seems that the nature of the functional group at the *ortho* position in the 1,3-aryl-triazenide ligands can be tuned in order to modulate the catalytic properties of their complexes. In addition, the chemoselective reduction of 6-methyl-5-hepten-2-one to 6-methyl-5-hepten-2-ol by complex **6** shows a promising area of opportunity to explore the catalytic properties of triazenide complexes on the selective transformation of other substrates containing two or more different functional groups.

Acknowledgements

This work was supported by Consejo Nacional de Ciencia y Tecnología (CONACyT) Grant 60467 and Dirección General de Educación Tecnológica (DGEST) Grant 5150.13-P. ECA thanks CONACyT for graduate fellowship. We thank CONACyT for ITT NMR and HRMS facilities (Grants INFR-2011-3-173395 and INFR-2012-01-187686).

Supplementary information

Supplementary NMR and RX Tables. Crystallographic data have been deposited at the Cambridge Crystallographic Data Center as supplementary material number CCDC 1438682 (**3**), 1437505 (**5**), 1438681 (**6**), 1437504 (**7**), 1439216 (**8**). Copies of the data can be obtained free of charge on application to CCDC, 12 Union Road, Cambridge CB2 1EZ, UK. E-mail:deposit@ccdc.cam.ac.uk.

References

[1] K. Vrieze, G. Van Koten, Comprehensive Coordination Chemistry, vol. 2, Pergamon Press, Oxford, UK, 1987.
[2] D.B. Kimball, M.M. Haley, Angew. Chem., Int. Ed. 41 (2002) 3338.
[3] D.V.Back, M. Hörner, F. Broch, G.M. Oliveira, Polyhedron 31 (2012) 558-564.
[4] A.P. Härter-Vaniel, A.E. Mauro, A.V.G. Netto, E. Tonon de Almeida, P.C. Piquini, P. Zambiazi, D.F. Back, M.J. Hörner, J. Mol. Struct. 1083 (2015) 311-318.

[5] T.V. Serebryanskaya, L.S. Ivashkevich, A.S. Lyakhov, P.N. Gaponic, Polyhedron 29 (2010) 2844-2850.
[6] L.Z. Fu, L.L. Zhou, S.Z. Zhan, Catal. Commun. 20 (2015) 26-29.
[7] M.Hörner, G. Manzoni de Oliveira, E.G. Koehler, L.D. Visentin, J. Organomet. Chem. 691 (2006) 1311-1314.
[8] A. Hinz, A. Schulz, A. Villinger, J.M. Wolter, J. Am. Chem. Soc. 137 (2015) 3975-3980.
[9] M.C. Barral, R. Gonzáles-Prieto, S. Herrero, L.J. Priego, E.C. Royer, M.R.Torres, F.A. Urbanos, J.A. Reyes, Polyhedron 23 (2004) 2637-2644.
[10] S. Ibañez, L. Oresmaa, F. Estevan, P. Hirva, M. Sanaú, M.A. Úbeda, Organometallics 33 (2014) 5378-5391.
[11] P. Gantzel, P.J. Walsh, Inorg. Chem. 37 (1998) 3450-3451.
[12] H.S. Lee, S.O. Hauber, D. Vindus, M. Niemeyer, Inorg. Chem. 47 (2008) 4401-4412.
[13] J.G. Rodríguez, M. Parra-Hake, G. Aguirre, F. Ortega, P.J. Walsh, Polyhedron 18 (1999) 3051.
[14] G. Ríos-Moreno, G. Aguirre, M. Parra-Hake, P.J. Walsh, Polyhedron 22 (2003) 563-568.
[15] C. Tejel, M.A. Ciriano, G. Ríos-Moreno, I.T. Dobrinovitch, F.J. LaHoz, L.A. Oro, M. Parra-Hake, Inorg. Chem. 43 (2004) 4719-4726.
[16] J.J. Nuricumbo-Escobar, C. Campos-Alvarado, G. Ríos-Moreno, D. Morales-Morales, P.J. Walsh, M. Parra-Hake, Inorg. Chem. 46 (2007) 6182-6189.
[17] J.J. Nuricumbo-Escobar, C. Campos-Alvarado, F. Rocha-Alonso, G. Ríos-Moreno, D. Morales-Morales, H. Höpfl, M. Parra-Hake, Inorg. Chim. Acta 363 (2010) 1150-1156.
[18] J. Sträle, C.F. Barboza, S. Schwarz, M.G. Mestres, S.T. López, S. T. *Z.* Anorg. Allg. Chem. 630 (2004) 1919-1923.
[19] G. Albertin, S. Antoniutti, J. Castro, S. Paganelli, J. Organomet. Chem.685 (2010) 2142-2152.
[20] J. Košmrlj, M. Osmak, D. Urankar, I. Piantanida, M. Matković, A. Ambriović-Ristov, A. Pevec, A. Brozovic, I. Steiner, J. Vajs, J. Inorg. Biochem. 153 (2015) 42-48.
[21] M.A. Bennett, T.N. Huang, T.W. Matheson, A.K. Smith, Inorg. Synth. 21 (1982) 74-75.
[22] A.E. Chichibabaín, R.L. Persitz, J. Russ. Phys. Chem. Soc. *57* (1925) 301-304.
[23] W.W. Hartman, J.B. Dickey, Org. Synth. 2 (1943) 163-165.
[24] G.M. Sheldrick, Acta Crystallogr. C**71** (2015) 3-8.
[25] *CrysAlis PRO* and *CrysAlis RED*. Agilent Technologies, Yarnton, **2013**.
[26] R.C. Clark, J.S. Reid, Acta Crystallogr., Sect. A: Found. Crystallogr. 51 (1995) 887-897.
[27] G. M. Sheldrick, Acta Crysallogr., Sect. A: Found. Crystallogr. 64 (2008) 112-122.
[28] L. Farrugia, J. Appl. Crystallogr. 30 (1997) 565.
[29] L. Farrugia, J. Appl. Crystallogr. *32* (1999) 837-838.
[30] G. Vernin, C. Siv, J. Metzger, C. Párkányi, Synthesis 10 (1977) 691.
[31]. M.R. Melardi, H.R.K. Ghaydar, M. Barkhi, M.K. Rofouei, Anal. Sci. 24 (2008) 281-282.
[32] M.K. Rofouei, M.R. Melari, Y. Salemi, J.A. Gharamaleki, Acta Crystallogr. *E65* (2009) o2391.
[33] J.A. Charamaleki, M.R. Melardi, S.M. Hosseini, F. Hosseinzadeh, M. Peyman, M.K. Rofouei, Polyhedron 44 (2012) 138-142.

[34] M.R. Melardi, A. Ghannadan, M. Peyman, G. Bruno, H. Amiri, Acta Crysallogr. E67 (2011) o3485.
[35] F. Rocha-Alonzo, G. Aguirre, M. Parra-Hake, Acta Crystallogr. E65 (2009) o990-o991.
[36] R. García-Álvarez, F.J. Suárez, J. Díez, P. Crochet, V. Cadierno, A. Antiñolo, R. Fernández-Galán, F. Carrillo-Hermosilla, Organometallics 31 (2012) 8301-8311.
[37] L. Menéndez-Rodríguez, E. Tomás-Mendivil, J. Francos, P. Crochet, V. Cadierno, A. Antiñolo, R. Fernández-Galán, F. Carrillo-Hermosilla, F. Organometallics 34 (2015) 2796-2809.
[38] T. Tsolis, M.J. Manos, S. Karkabounas, I. Zelovitis, A. Garaufis, J. Organomet. Chem. 768 (2014) 1-9.
[39] L.D. Brown, J.A. Ibers, Inorg. Chem. 15 (1976) 2788-2793.
[40] A. Chakravorty, M. Bag, S. Chattopadhyay, A. Prammanik, M. Menon, Inorg. Chem. 34 (1995) 1361-1367.
[41] L.D. Brown, J.A. Ibers, Inorg. Chem. 34 (1995) 1361-1367.
[42] G. Albertin, S. Antoniutti, M. Bedin, J. Castro, S. Garcia-Fontán, S. Inorg. Chem. 45 (2006) 3816-3835.
[43] M.B. Hursthouse, M.A. Mazid, T. Clark, S.D. Robinson, Polyhedron 12 (1993) 563-565.
[44] T. Clark, J. Cochrane, S.F. Colson, K.Z. Malik, S.D. Robinson, J.W. Steed, Polyhedron 20 (2001) 1875–1880.
[45] N.S. Chowdhury, C. Guharoy, R.J. Butcher, S. Bhattacharya, Inorg. Chim. Acta 406 (2013) 20-26.
[46] T. Singh, R. Kishan, M. Nethaji, N. Thirupathi, Inorg. Chem. 51 (2012) 157-169.
[47] S.E. Clapham, A. Hadzovic, R. H. Morris, Coord. Chem. Rev. 248 (2004) 2201-2237.

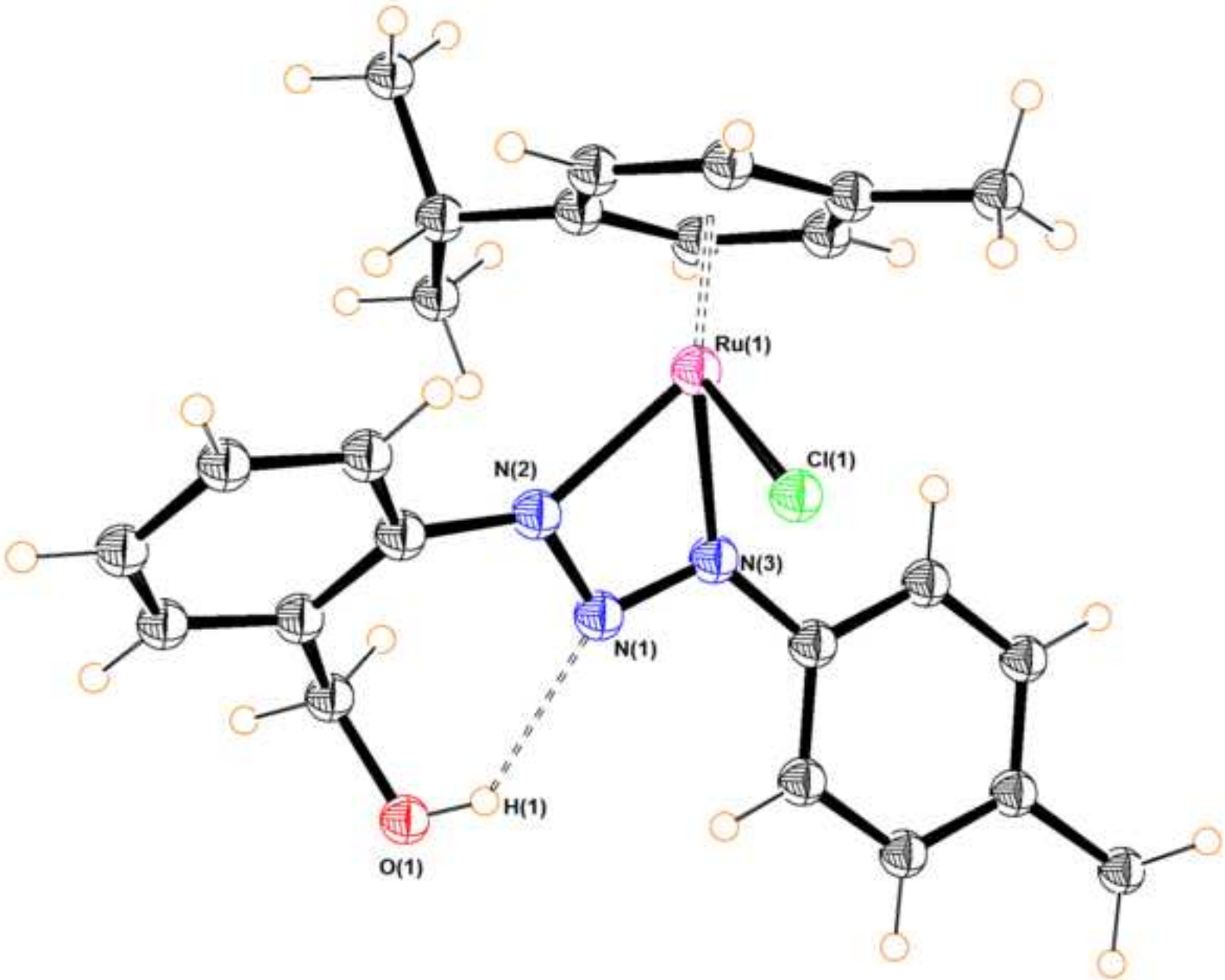
Ru(1)
Cl(1)
N(2)
N(3)
N(1)
H(1)
O(1)

Highlights

Ruthenium triazenide complexes as selective catalysts for hydrogenation of alkenones.

Intramolecular hydrogen bonding in triazenes and ruthenium triazenide complexes.

Base free transfer hydrogenation by ruthenium triazenide complexes.